Effect of Attapulgite Contents on Release Behaviors of a pH Sensitive Carboxymethyl Cellulose-*g*-Poly(acrylic acid)/Attapulgite/Sodium Alginate Composite Hydrogel Bead Containing Diclofenac

Qin Wang,[1] Wenbo Wang,[1] Jie Wu,[2] Aiqin Wang[1,2]

[1]*Center of Eco-material and Green Chemistry, Lanzhou Institute of Chemical Physics, Chinese Academy of Sciences, Lanzhou 730000, People's Republic of China*
[2]*Key Laboratory of Attapulgite Science and Applied Technology of Jiangsu Province, Huaiyin Institute of Technology, Huaian 223003, People's Republic of China*

Received 6 November 2010; accepted 7 August 2011
DOI 10.1002/app.35440
Published online 2 December 2011 in Wiley Online Library (wileyonlinelibrary.com).

ABSTRACT: A series of pH-sensitive composite hydrogel beads, carboxymethyl cellulose-*g*-poly(acrylic acid)/attapulgite/sodium alginate (CMC-*g*-PAA/APT/SA), were prepared by combining CMC-*g*-PAA/APT composite and SA, using Ca^{2+} as the ionic crosslinking agent and diclofenac sodium (DS) as the model drug. The effects of APT content and external pH on the swelling properties and release behaviors of DS from the composite hydrogel beads were investigated. The results showed that the composite hydrogel beads exhibited good pH-sensitivity. Introducing 20% APT into CMC-*g*-PAA hydrogel could change the surface structure of the composite hydrogel beads, decrease the swelling ability, and relieve the burst release effect of DS. The drug cumulative release ratio of DS from the hydrogel beads in simulated gastric fluid was only 3.71% within 3 hour, but in simulated intestinal fluid about 50% for 3 hour, 85% for 12 hour, up to 90% after 24 hour. The obtained results indicated that the CMC-*g*-PAA/APT/SA hydrogel beads could be applied to the drug delivery system as drug carriers in the intestinal tract. © 2011 Wiley Periodicals, Inc. J Appl Polym Sci 124: 4424–4432, 2012

Key words: composite hydrogel; carboxymethyl cellulose; attapulgite; pH-sensitive; controlled release

INTRODUCTION

Various natural and/or synthetic polymers have been adopted for drug delivery system due to their excellent properties such as biocompatibility, biodegradability and long-term safety of drugs.[1,2] However, using single natural polymers as a drug carrier may cause the instability of drug owing to its water-solubility and degradability.[3,4] Clay minerals, include smectites, palygorskite, kaolinite and talc, have a high specific area and absorptive capacity, rheological properties and low or null toxicity and are usually used in Pharmaceutical Technology and Dermopharmacy as ideal excipients and substances of suitable biological activity.[5,6] In addition, clays are also used to delay and/or target drug release or even improve drug dissolution and simultaneously increase drug stability.[7–9] However, these clays have poor sensibility to changes in external conditions such as pH, temperature and electric currents, etc.[9]

In order to resolve the above shortcomings of pure polymer or clays in drug delivery system, new strategies are reported that clays have been introduced into polymer by different methods.[10–12] It was found that the introduction of versatile inorganic materials could not only remedy some flaws of the neat polymers but also often endow them with novel properties.[13,14] For instance, biopolymer/montmorillonite nanocomposite exhibited higher drug-loaded capacity and better drug controlled release properties in the case of certain MMT incorporation.[15] Chitosan/organic rectorite nano-composite films displayed good mechanical property, antiultraviolet capacity and bactericidal activity by introducing organified rectorite.[16] The introduction of layered double hydroxides into sodium alginate (SA) could restrict the movability of the SA polymer chains and then slow down swelling and dissolution rates of the hybrid beads in aqueous solutions.[17] In addition, these polymer/clay composites also showed good sensibility.

Carboxymethyl cellulose (CMC), an anionic derivative of cellulose, attracts more and more attention

Correspondence to: A. Wang (aqwang@licp.cas.cn).
Contract grant sponsor: Jiangsu Provincial Science and Technology Office; contract grant number: BE2009098.
Contract grant sponsor: Special Research Fund of Scholarship of Dean of CAS.

recently as raw materials for the design of drug delivery formulations because of its advantages of good water-solubility, high abundance and low price.[18,19] CMC with chemically reactive groups (primary, secondary —OH and —COOH) can be easily modified by chemical reaction.[20–23] So, in this article, novel carboxymethyl cellulose-*g*-poly(acrylic acid)/attapulgite (CMC-*g*-PAA/APT) nanocomposites with different amounts of APT were synthesized through free-radical graft-copolymerization among CMC, APT, and AA, which exhibited excellent pH-sensitivity.[24] The resultant composite was then combined with sodium alginate (SA) by Ca^{2+} ionic crosslinking to form a series of composite hydrogel beads. Swelling and pH sensitive characteristics of the CMC-*g*-PAA/APT/SA composite hydrogel beads were discussed. Furthermore, the controlled drug delivery behaviors of hydrogel beads were investigated by using diclofenac sodium (DS) as the model drug in detail.

EXPERIMENTAL

Materials

Acrylic acid (AA, distilled under reduced pressure before use), ammonium persulfate (APS, analytical grade, recrystallized from distilled water before use) and *N, N′*-methylenebisacrylamide (MBA, analytical grade) were purchased from Shanghai Reagent (Shanghai, China). Sodium carboxymethyl cellulose (CMC) was purchased from Sinopharm Chemical Reagent (Shanghai, China). Attapulgite (APT, a type of clay) was supplied by Jiuchuan Colloidal, (Jiangsu, China). Sodium alginate (SA) was purchased from Shanghai Chemical (China). Diclofenac sodium (DS) was purchased from Jiuzhou pharmaceutical factory (He'nan, China). All the other reagents used were of analytical grade and all solutions were prepared with distilled water.

Preparation of CMC-*g*-PAA/APT nanocomposites

CMC-*g*-PAA/APT nanocomposites were prepared according to our previous reports.[24] CMC powder (1.03 g) was dissolved in 30 mL distilled water in a 250-mL four-necked flask equipped with a mechanical stirrer, a thermometer, a reflux condenser and a nitrogen line to form a transparent sticky solution. The solution was heated to 60°C and deoxygened by purging with N_2 for 30 min. Then, 5 mL of aqueous solution of initiator APS (0.072 g) was added under continuous stirring and kept at 60°C for 10 min to generate radicals. Acrylic acid (AA) (7.2 g) was neutralized by 7.6 mL 8.8 mol/L NaOH solution, and fully mixed with 18 mg crosslinker, (MBA) and calculated amount of APT powder (0.44 g, 5 wt %; 0.95 g, 10 wt %; 2.08 g, 20 wt %; 2.78 g, 25 wt %) under magnetic stirring. After cooling the reactants to 50°C, the mixture was added into the flask and the temperature was risen to 70°C and maintained for 3 hour to complete reaction. A nitrogen atmosphere was maintained throughout the reaction period. The obtained nanocomposites were washed with distilled water for several times and dried to constant weight at 70°C, ground and sieved to 40–80 mesh (180–380 μm). CMC-*g*-PAA hydrogels were prepared according to a similar procedure except without addition of APT.

Preparation of CMC-*g*-PAA/APT/SA composite hydrogel beads

A series of CMC-*g*-PAA/APT/SA composite hydrogel beads was prepared as follows. DS (0.50 g) was dissolved in 150 mL of distilled water in a 250 mL flask using a mechanical stirrer (200 rpm for 30 min), and then 1.00 g of CMC-*g*-PAA/APT particles (<120 mesh) was charged into the flask. The mixture was stirred for 3 hour to facilitate the penetration of DS molecules into CMC-*g*-PAA/APT hydrogel. Subsequently, a predetermined amount of SA was added into the above mixture and was further stirred at 1000 rpm for 4 hour to ensure homogeneity of the mixture. The mixture was dropped into 200 mL $CaCl_2$ solution through a 0.45 mm syringe needle at a dropping rate of 1.50 mL min^{-1}. Composite hydrogel beads were allowed to crosslink with Ca^{2+} in solution for 2 hour. The obtained composite hydrogel beads were rinsed with distilled water for three times to remove unreacted $CaCl_2$ on surface and subsequently dried at 80°C in an oven.

Swelling ratio test

Swelling properties of DS-loaded CMC-*g*-PAA/APT/SA composite hydrogel beads were carried out in pH 6.8 phosphate buffer solution (PBS). The composite hydrogel beads (0.10 g) were placed in the baskets of intelligent dissolution apparatus (ZRS-8G, Tianjing University Wireless factory, China) containing 200 mL of pH 6.8 PBS and stirred at 37°C ± 1°C at 50 rpm. At predetermined intervals of time, the composite hydrogel beads were taken out using a 0.14 mm screen and weighed after carefully wiping off residual liquid with a tissue paper. The swelling ratio is evaluated using the following equation:

$$\text{Swelling ratio} = (W_s - W_d)/W_d \quad (1)$$

where W_s and W_d is the swollen and dry weight of composite hydrogel beads at time t, respectively. Swelling ratio in solutions of various pH values was tested according to the same procedure. The buffer solutions of various pH values were made by properly combining NaH_2PO_4, Na_2HPO_4, NaCl and

NaOH solutions. Ionic strengths of all the buffer solutions were adjusted with 0.2 mol/L NaCl solution. The pH values were determined with a pH meter (DELTA-320).

Determination of encapsulation efficiency and drug loading

DS-loaded composite hydrogel beads (0.10 g) was immersed in 10 mL of pH 6.8 PBS in a 50 mL beaker for completely swelling. The swollen beads were crushed in an agate mortar with a pestle and transferred into a conical flask, and then about 20 mL of the fresh PBS was added to the conical flask and the homogeneous mixture was sonicated for 20 min. The DS solution was separated from the mixture after being centrifuged for 20 min at 5000 rpm. The amount of DS was determined using UV-vis spectrophotometer (SPECORD 200, ANALYTIK JENA AG). The drug loading (%) and encapsulation efficiency (%) were calculated using the following equations, respectively:

$$\text{Drug loading (\%)} = \frac{\text{Weight of drug in hydrogel beads}}{\text{Weight of hydrogel beads}} \times 100 \quad (2)$$

$$\text{Encapsulation efficiency (\%)} = \frac{\text{Weight of drug in hydrogel beads}}{\text{Theoretical drug loading}} \times 100 \quad (3)$$

In vitro drug release

In vitro release experiments were carried out using an intelligent dissolution apparatus by immersing 0.50 g of the dried DS-loaded CMC-*g*-PAA/APT/SA composite hydrogel beads in 500 mL dissolution medium. The dissolution media (pH 2.1 or 6.8) were prepared by combining HCl, KH_2PO_4 and NaOH solution properly according to the Chinese Pharmacopoeia 2005. The mixture was stirred at 50 rpm and kept at 37°C ± 1°C. At predetermined time intervals, 5 mL of the solution was taken and the same amount of the fresh PBS was added back to maintain a constant volume. The collected 5 mL of the solution was filtrated through a membrane with a pore diameter of 0.45 μm. The filtrate (3 mL) was diluted to 25 mL with the fresh PBS. The concentration of DS was determined by a UV-vis spectrophotometer at 280 nm, and then the cumulative percentage of DS released was obtained. The dissolution results were the average of three measurements.

Characterization

FTIR spectra of the hydrogel beads were taken as KBr pellets using a Thermo Nicolet NEXUS TM spectrophotometer. Micrographs of the hydrogel beads were taken using scanning electron microscopy (JSM-5600LV, JEOL) after coating the sample with gold film.

Statistical analysis

Statistical analysis for the determination of differences in the swelling and release characteristics within groups was accomplished using one-way analysis of variance, performed with a statistical program (SPSS 13.0 for Windows). The data were considered to be significantly different at $P < 0.05$. All data are presented as mean values with standard error (mean ± SE).

RESULTS AND DISCUSSION

Preparation and characteristics of CMC-*g*-PAA/APT/SA composite hydrogel beads

The existence of chemically reactive —OH groups of APT makes it easily react with CMC and AA under certain conditions, and then form CMC-*g*-PAA/APT nanocomposites with three-dimensional network structure. This nanocomposites exhibited excellent hydrophilic property and adsorption capacity.[24,25] In this work, CMC-*g*-PAA/APT nanocomposites as drug carriers were first studied to extend its application fields. However, it was found in preliminary experiments that the burst effect of drug loaded in the nanocomposites was very obvious in pH 6.8 PBS. Hence, CMC-*g*-PAA/APT/SA hydrogel beads were prepared by ionic gelation in order to reduce the burst release of drug loaded.

To prove the interaction between DS and CMC-*g*-PAA/APT/SA, the FTIR spectra of (a) DS, (b) CMC-*g*-PAA/APT/SA, and (c) DS-loaded CMC-*g*-PAA/APT/SA composite hydrogel beads are shown in Figure 1. In Figure 1(b), the strong absorption bands of CMC-*g*-PAA/APT/SA composite beads at 1707 cm^{-1} and 1420 cm^{-1} are attributed to the asymmetric stretching vibration of —COOH and the asymmetric stretching vibration of $—COO^-$ groups, respectively. As DS molecules are introduced into the CMC-*g*-PAA/APT/SA composite hydrogels, the absorption band of CMC-*g*-PAA/APT/SA at 1707 cm^{-1} was shifted to 1694 cm^{-1} in Figure 1(c), indicating the interactions between DS and CMC-*g*-PAA/APT/SA matrix. This may be attributed to the ionic bonding between $—COO^-$ groups of DS molecules and Ca^{2+} ions in CMC-*g*-PAA/APT/SA hydrogel beads, and the electrostatic interaction of DS and SA.[26] Moreover, the strong absorption bands at 1507 cm^{-1} and 1453 cm^{-1} on DS molecule [Fig. 1(a)] appear in the spectrum of DS-loaded CMC-*g*-PAA/APT/SA with a slight shift, which indicates the successful entrapment of DS. In addition, no extra peaks

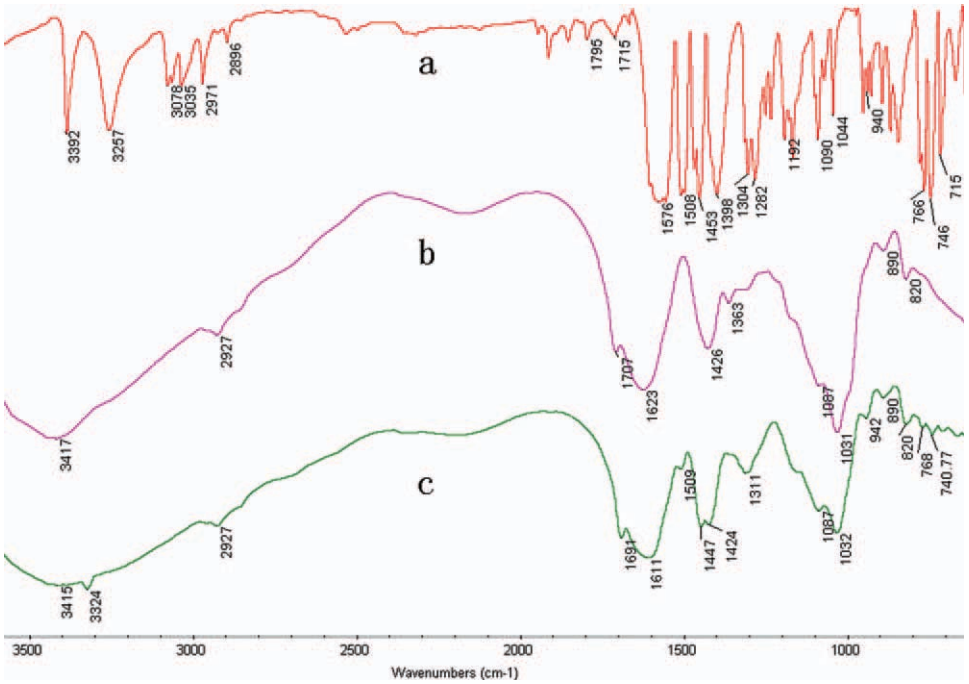

Figure 1 FTIR spectra of (a) DS, (b) CMC-*g*-PAA/APT/SA, and (c) DS-loaded CMC-*g*-PAA/APT/SA. [Color figure can be viewed in the online issue, which is available at wileyonlinelibrary.com.]

can be seen from Figure 1(c), indicating that the molecular structure of DS loaded in hydrogel beads has not been damaged during the experiment. This result was also supported by the maximum wavelength of DS using UV-vis spectrophotometer mensuration in Figure 2. As can be seen from Figure 2, when DS molecules were encapsulated, the maximum wavelength of DS shown in Figure 2(b) was in accordance with that of DS unencapsulated shown in Figure 2(a). This further proved that DS molecules were well entrapped in the hydrogel beads without any chemical deterioration of functional groups.

To show the influence of APT on CMC-*g*-PAA/SA hydrogel beads directly, thus, the morphology of CMC-*g*-PAA/APT/SA composite hydrogel beads was also investigated in this section and is shown in Figure 3. As can be seen from Figure 3(a), most of the spherical DS-loaded CMC-*g*-PAA/APT/SA composite hydrogel beads showed a smooth surface, and the size at swollen state is around 4.0–5.0 mm. After dried at the room temperature, the sizes of the beads are approximate 2 mm in Figure 3(b). Comparing Figure 3(c) with (d–g), it can be discovered that the surface of CMC-*g*-PAA/SA composite hydrogel bead is compact [Fig. 3(c)]; when 5% APT content was introduced into the CMC-*g*-PAA/SA matrix, the surface of CMC-*g*-PAA/APT/SA composite hydrogel bead was hardly changed [Fig. 3(d)]; however, increasing APT content from 10 to 25 wt %, the CMC-*g*-PAA/APT/SA composite hydrogel bead shows a loose and lacunaris surface [Fig. 3(e–g)], which may have some influences on the swelling abilities of the composite hydrogel beads and the release behaviors of DS from the composite hydrogel beads.

Effect of weigh ratio of CMC-*g*-PAA/APT to SA on swelling ratio

Figure 4 shows the swelling characteristics of CMC-*g*-PAA/APT/SA composite hydrogel beads at various ratio of CMC-*g*-PAA/APT to SA. In pH 6.8 PBS, the swelling ratio of the composite hydrogel beads increase with increasing the weight ratio of CMC-*g*-

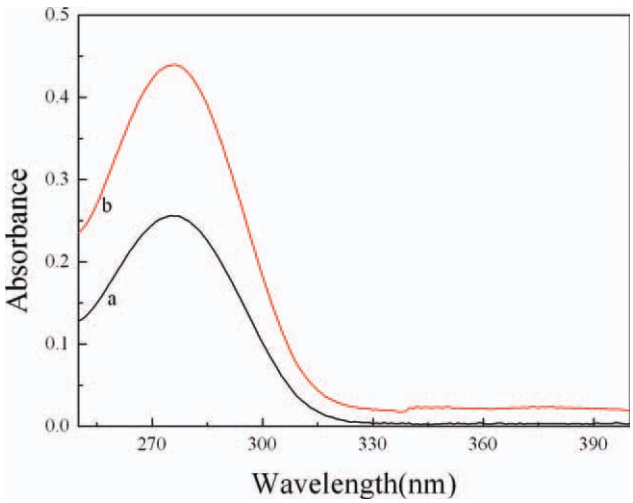

Figure 2 UV-vis spectra of (a) unencapsulated DS and (b) encapsulated DS. [Color figure can be viewed in the online issue, which is available at wileyonlinelibrary.com.]

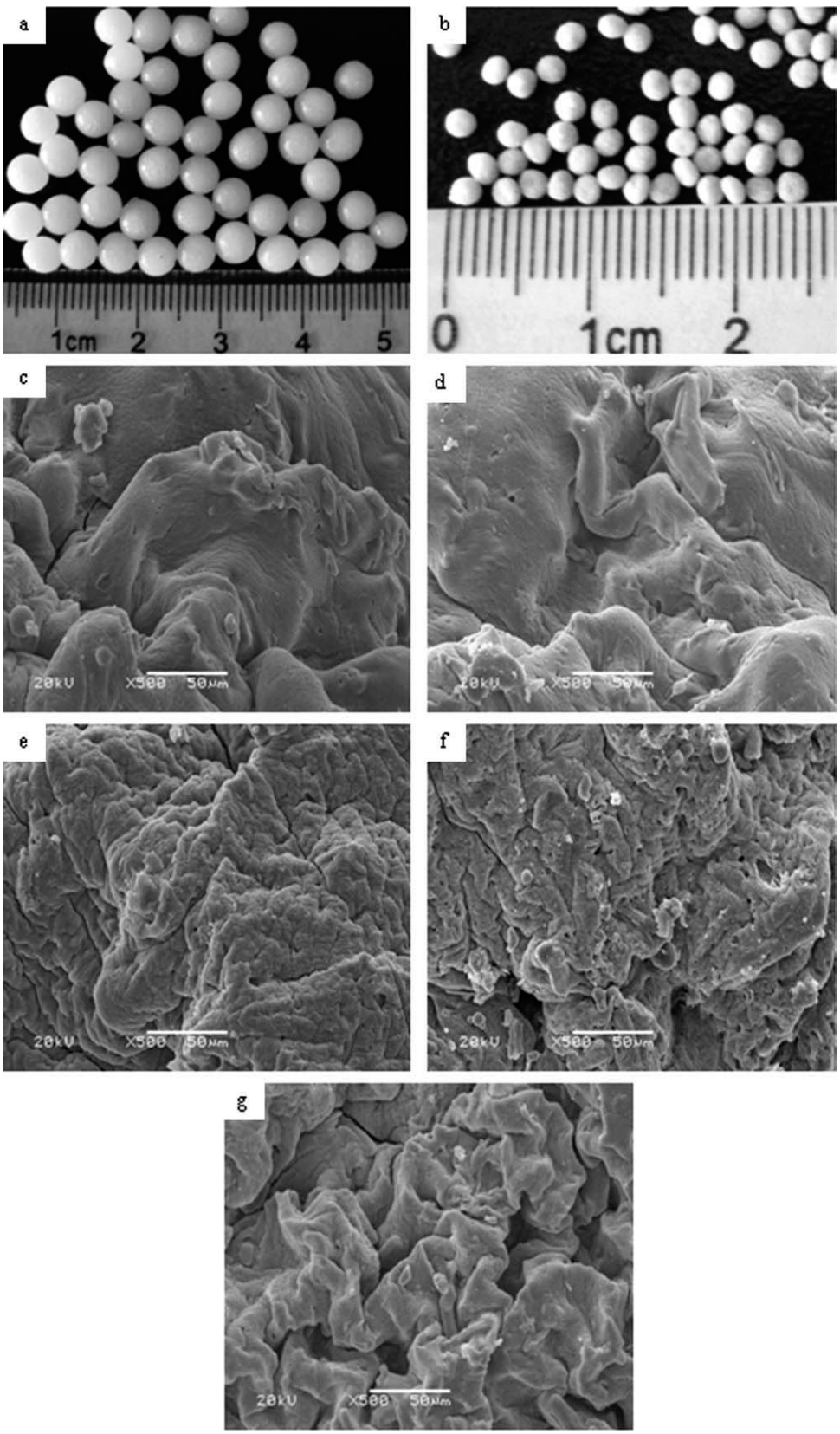

Figure 3 Digital photos of (a) DS-loaded CMC-*g*-PAA/10%APT/SA composite hydrogel beads at a swollen state and (b) DS-loaded CMC-*g*-PAA/10%APT/SA composite hydrogel beads at a dry state. SEM images of (c–g) CMC-*g*-PAA/APT/SA composite hydrogel bead with different APT content (c: 0 wt %, d: 5 wt %, e:10 wt %, f: 20 wt %, and g: 25 wt %, respectively) (×500).

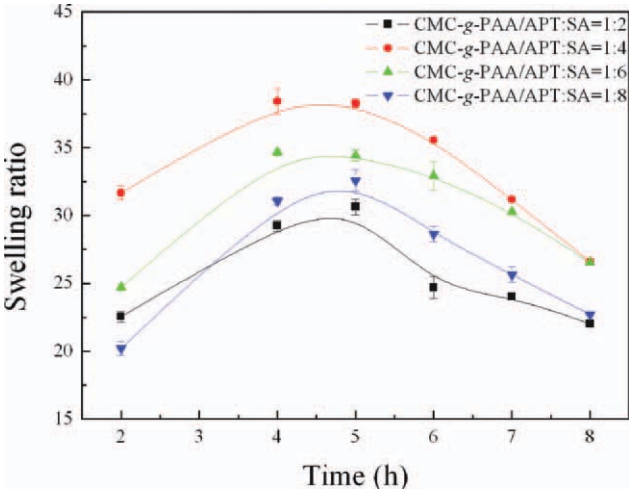

Figure 4 The influence of weight ratio of CMC-*g*-PAA/APT to SA on the swelling ratio for CMC-*g*-PAA/APT/SA composite hydrogel beads at pH 6.8 PBS. Data are presented as means ± SD ($n = 3$). [Color figure can be viewed in the online issue, which is available at wileyonlinelibrary.com.]

PAA/APT to SA at the same time except for 1 : 2 ratio (CMC-*g*-PAA/APT: SA) ($P < 0.05$).

It is known that the contact between SA and Ca^{2+} in solution immediately induces ionic crosslinking of SA, and then forms a hydrogel bead.[27] CMC-*g*-PAA/APT is actually a composite polymer containing numerous hydroxyl and carboxyl groups. The —COO^- groups of CMC-*g*-PAA/APT and SA can complex with the Ca^{2+} ions in solution and generate —COO...Ca...OOC— ionic crosslinkages. Therefore, CMC-*g*-PAA/APT nanocomposites could be connected to SA polymer chains by Ca^{2+} crosslinking interaction, and formed a new network composed of CMC-*g*-PAA/APT and SA. The interactions between CMC-*g*-PAA/APT and SA by Ca^{2+} crosslinking were strengthened with increasing the amount of SA, which make the new network closer and then result in decrease of swelling ratio. But at the ratio of 1 : 2, the swelling ratio was lower than that of the other hydrogel beads. This result may be attributed to the following fact. At the ratio of 1 : 2, the crosslinking interaction between CMC-*g*-PAA/APT and SA by Ca^{2+} ions was relatively weaker because of the less amount of SA, and the formed composite hydrogel beads are easily broken. Thus, the swelling ratio was decreased due to the leakage of the microparticles (generated owing to crack of the beads) smaller than 0.14 mm. This difference of swelling ability with changing SA content may have some influences on the release of DS from the composite hydrogel beads.

In addition, as can be also seen from Figure 4, the swelling ratio increases with increasing time at the initial 2–5 hour, which is attributed to the expansion of the hydrogel network and the penetration of water molecules. The decreasing tendency of swelling ratio with further increasing time is attributed to the following facts. There are three kinds of anions ($H_2PO_4^-$, HPO_4^{2-}, and PO_4^{3-}) in pH 6.8 PBS, PO_4^{3-} ions may reacts with Ca^{2+} ions to form a precipitation, which disrupt the ionic crosslinking in the beads and make the hydrogel beads crack gradually, and then resulting in the decrease of the swelling ratio with further the increase of time.

Effect of $CaCl_2$ concentration on swelling ratio

Figure 5 shows the swelling curves of CMC-*g*-PAA/APT/SA composite hydrogel beads prepared at different concentrations of $CaCl_2$. It is observed that the higher the $CaCl_2$ concentration, the smaller the swelling ratio of the composite hydrogel beads. This can be easily explained by the fact that a higher $CaCl_2$ concentration generates a more compact hydrogel structure, which results in a closer and stronger bonding between CMC-*g*-PAA/APT and SA. The variation of swelling ratio with $CaCl_2$ concentration may also be beneficial to the drug controlled release.

Effect of APT content on swelling ratio

Figure 6 showed the effect of APT content on swelling ratio of the CMC-*g*-PAA/APT/SA composite hydrogel beads in pH 6.8 PBS. It is obvious that APT content is an important factor affecting swelling ratio. The swelling ratio increases with an increase in APT content until reaching a maximum at 10 wt % ($P < 0.05$). APT is rigid and contains large amounts of active —OH groups on its surface, which

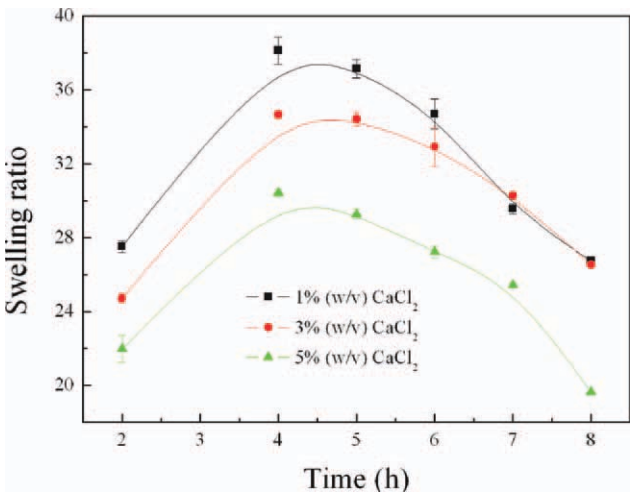

Figure 5 The influence of $CaCl_2$ concentration on the swelling ratio for CMC-*g*-PAA/APT/SA composite hydrogel beads at pH 6.8 PBS. Data are presented as means ± SD ($n = 3$). [Color figure can be viewed in the online issue, which is available at wileyonlinelibrary.com.]

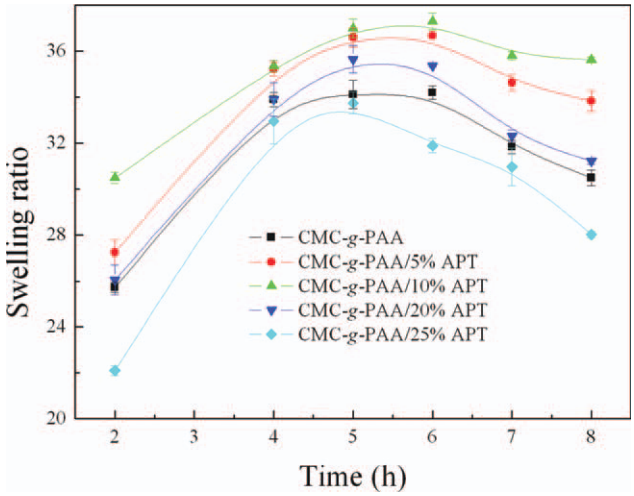

Figure 6 The influence of APT content on the swelling ratio for CMC-*g*-PAA/APT/SA composite hydrogel beads at pH 6.8 PBS. Data are presented as means ± SD ($n = 3$). [Color figure can be viewed in the online issue, which is available at wileyonlinelibrary.com.]

can take part in the polymerization reaction as well as the construction of 3D network. As a result, the intertwining of polymeric chains was prevented and the hydrogen-bonding interaction between hydrophilic groups such as —COOH, —COO^-, and —OH, etc. was weakened. Thus, the degree of physical crosslinking decreased and the network voids for holding water regularly formed; this is extremely favorable to the improvement of swelling ratio.[24]

It was also noticed from Figure 6 that the swelling ratio decreased when APT content exceeded 10 wt % ($P < 0.05$). According to previous report,[28] ultrafine clay powder may act as additional crosslinking points in polymer networks. The chemical composite

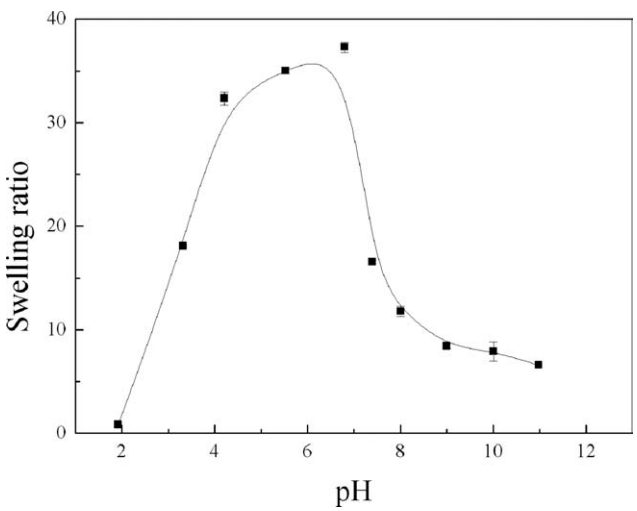

Figure 7 Variation of swelling ratio for CMC-*g*-PAA/APT/SA composite hydrogel beads at different pH solution. Data are presented as means ± SD ($n = 3$).

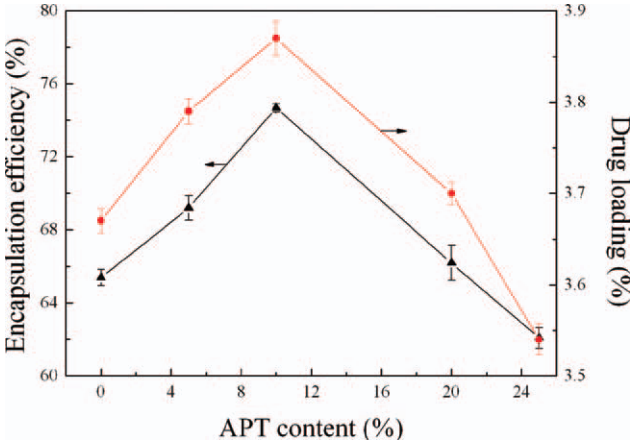

Figure 8 Loading of DS into CMC-*g*-PAA/APT/SA composite hydrogel beads with different APT content (wt %). Data are presented as means ± SD ($n = 3$). [Color figure can be viewed in the online issue, which is available at wileyonlinelibrary.com.]

of APT with polymeric matrix enhanced the crosslinking density of nanocomposite and minimized the network voids for absorbing and holding water. In addition, the excessive APT particles may physically stack in the network voids. On the one hand, some voids were plugged up and the water-holding capability decreased; on the other hand, the filling of excess APT decreased the ratio of hydrophilic groups in unit volume and the hydrophilicity of nanocomposite. Consequently, the swelling ratio decreased with the increase of APT content above 10 wt %. A similar tendency was also observed by Li et al.[29]

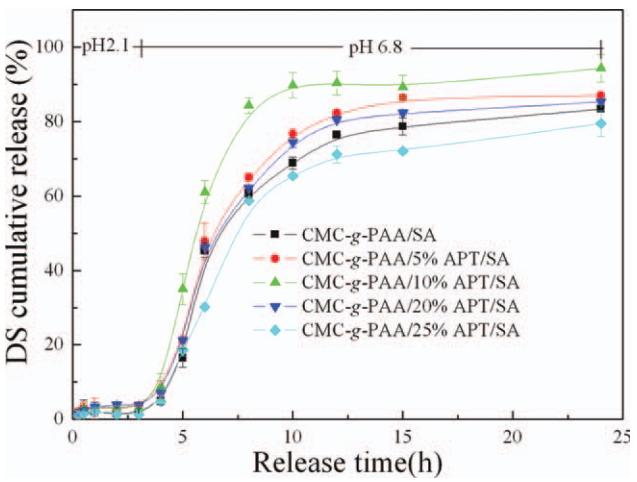

Figure 9 *In vitro* cumulative release profiles of DS from CMC-*g*-PAA/APT/SA composite hydrogel beads with different APT content in simulated gastric fluid (pH 2.1 PBS, first 3 hour) and simulated intestinal fluid (pH 6.8 PBS) at 37°C. Data are presented as means ± SD ($n = 3$). [Color figure can be viewed in the online issue, which is available at wileyonlinelibrary.com.]

TABLE I
Drug Release Mechanism of DS Loaded CMC-*g*-PAA/APT/SA Composite Hydrogel Beads

Samples	n^a	k^b	r^{2c}	Drug release mechanism
CMC-*g*-PAA/SA	0.498 ± 0.033	0.272 ± 0.023	0.960	Anomalous transport
CMC-*g*-PAA/5%APT/SA	0.632 ± 0.047	0.231 ± 0.013	0.983	Anomalous transport
CMC-*g*-PAA/10%APT/SA	0.782 ± 0.021	0.207 ± 0.080	0.982	Anomalous transport
CMC-*g*-PAA/20%APT/SA	0.963 ± 0.008	0.147 ± 0.001	0.950	Case-II transport
CMC-*g*-PAA/25%APT/SA	1.271 ± 0.062	0.064 ± 0.007	0.918	Case-II transport

[a] Diffusional exponents.
[b] Kinetic constants.
[c] Correlation coefficients. Data are presented as means ± SD ($n = 3$), ($P < 0.05$).

Effect of pH on swelling ratio

pH dependence of the maximum swelling ratio is shown in Figure 7. It can be observed from Figure 7 that the swelling ratio increases sharply to 37.3 ± 0.49 with increasing pH from 2.0 to 6.8, and then decreases evidently to 6.59 ± 0.11 with further increasing the pH to 11.0. The onset pH value of the shrinkage of the swollen composite hydrogel beads lied around pH 6.8. When pH $\leq$ 2.0, —COO^- groups convert to —COOH groups, and then hydrogen bonding between —COOH groups and —OH groups of CMC-*g*-PAA/APT/SA formed, this is responsible for the small swelling ratio. As pH increases gradually to 6.8, most of —COOH groups transformed into —COO^- groups and the hydrogen bonding dissociated. Thus, the electrostatic repulsion within the test hydrogel beads makes the hydrogel swell more. However, when pH > 6.8, the swelling ratio decrease evidently. The result may be mostly ascribed to the dissolution of SA and the rupture of the composite hydrogel beads due to the reaction of PO_4^{3-} and Ca^{2+} ions in the basic region.[30] The characteristic for the variation of swelling ratio with pH of external buffer solution indicates good pH-sensitive behavior of the CMC-*g*-PAA/APT/SA composite hydrogel beads.

Drug loading of the composite hydrogel beads

For a drug carrier, the high loading capacity for drug is a desirable property. Thus, in this section the effects of APT content on the encapsulation efficiency and the drug loading of the composite hydrogel beads were investigated and are shown in Figure 8. As can be seen, the incorporation of APT in the beads very effectively increase the entrapment of DS when APT content $\leq$10 wt % ($P < 0.05$), but then decrease with further increasing the content of APT. This result may be attributed to the following reasons. First, APT contains plentiful active –OH groups on its surface, which can participate in the polymerization reaction, forming a three-dimensional network structure. The incorporation of APT can relieve the physical entanglement of the grafted polymeric chains and weaken the hydrogen-bonding interaction among hydrophilic groups, which decreases the physical crosslinking degree and improves the polymer network. This improved polymer network is helpful to the immigration of drug. Consequently, the higher encapsulation efficiency and the drug loading were observed. Second, further increasing the APT content from 10 to 25 wt %, the additional APT may produce more crosslinking points in polymer network and minimize the network space for DS, and then resulting in the decrease of the encapsulation efficiency and the drug loading. Li et al also found that the encapsulation efficiency of CMC/clay for acetochlor increased first and then decreased with increasing the content of clay.[31]

Controlled drug release

The different types of the composite hydrogel beads in terms of APT content were compared with respect to the release of DS in simulated gastric fluid and simulated intestinal fluid. The cumulative percentage of DS released from the composite hydrogel beads was plotted as a function of time in Figure 9. Obviously, only a tiny amount of DS releases from the matrix and the release rate of all test groups with different APT content had no distinct difference ($P > 0.05$). However, DS releases quickly after being transferred into simulated intestinal fluid and above 90% of entrapped DS was released for 6 hour. The very low release percentage at pH 2.1 may be ascribed to the following facts: (i) DS is weak acid salt and it has very low solubility in an acidic medium. So it can not release in this medium; (ii) SA can convert to alginic acid (insoluble form) in dilute acid medium, which makes the hydrogel beads not splinter easily; (iii) the shrinking behavior of the composite beads can make DS not release (Fig. 7). Whereas, the quick release of DS at pH 6.8 PBS is due to the higher swelling and the breaking of the composite hydrogel beads. Therefore, these results indicate that the CMC-*g*-PAA/APT/SA composite hydrogel beads are good candidates as a drug delivery system in the intestinal tract.

In addition, from Figure 9 it was also found that the DS cumulative release ratio from CMC-*g*-PAA/APT/SA composite hydrogel beads increases firstly, and then decreases with the increase of APT content in simulated intestinal fluid ($P < 0.05$). This may be attributed to the follow facts: (1) the difference of the swelling ratio of CMC-*g*-PAA/APT/SA composite hydrogel beads with different APT content. The higher swelling ratio usually corresponds to a better elasticity of the polymer chains and a larger network space, and so DS can emigrate out of the composite hydrogel beads more easily; (2) the difference of DS release mechanism. To compare the differences on the release of DS from the composite hydrogel beads with different amounts of APT, the release data were analyzed by applying the empirical eq. (4) proposed by Ritger and Peppas[32]:

$$M_t/M_\infty = kt^n \quad (4)$$

where M_t/M_∞ is the ratio of drug released at time t, k is a constant that incorporates the characteristics of the carrier and the drug, and n is a parameter that is indicative of the transport mechanism. Table I presents the calculated values of k and n parameters of the cumulative release data of DS loaded in the composite hydrogel beads with different APT content by empirical eq.(4). The n values gradually increase from 0.498 ± 0.033 to 1.271 ± 0.062 with increasing the content of APT from 0 to 25 wt %. For a sphere, when $n < 0.43$, this represents a Fickian diffusion mechanism. When $n > 0.86$, this represents a Case II transport mechanism. When n value is between 0.43 and 0.86, the transport is a typical and both Fickian diffusion and Case II transport contribute to the release, i.e., anomalous transport. In our experiments, the n values are between 0.43 and 0.86 when APT content ≤10 wt %, this indicates that DS was released by a combination of Fickian diffusion and Case-II transport processes. When APT content >10 wt %, the n values were larger than 0.86, indicating that DS was released by a Case-II transport process.

CONCLUSIONS

The novel pH-sensitive CMC-*g*-PAA/APT/SA composite hydrogel beads were successfully prepared using ionic gelation method. The results of IR and UV indicated that DS could disperse in the CMC-*g*-PAA/APT/SA composite hydrogel beads, and its molecular structure has not been damaged during the experiment. SEM observation indicates that the composite hydrogel beads have a microporous surface morphology when the content of APT introduced exceeds 5 wt %, which may be benefit for the immigration and emigration of drug. The release data showed that a sustained release can be obtained in simulated intestinal fluid, and the CMC-*g*-PAA/APT/SA hydrogel beads can be applied to the drug delivery system as drug carriers in the intestinal tract.

References

1. Amass, W.; Amass, A.; Tighe, B. Polym Int 1998, 47, 89.
2. Kumari, A.; Yadav, S. K.; Yadav, S. C. Colloid Surf B 2010, 75, 1.
3. Sinha, V. R.; Trehan, A. J Controlled Release 2003, 90, 261.
4. Soppimath, K. S.; Aminabhavi, T. M.; Kulkarn, A. R.; Rudzinski, W. E. J Controlled Release 2001, 70, 1.
5. Caia, P.; Zhu, J.; Huang, Q. Y.; Fang, L. C.; Liang, W.; Chen, W. L. Colloids Surf B 2009, 69, 26.
6. López-Galindo, A.; Viseras, C.; Cerezo, P. Appl Clay Sci 2007, 36, 51.
7. Gasser, M. S. Colloids Surf B 2009, 73, 103.
8. Viseras, C.; Cerezo, P.; Sanchez, R.; Salcedo, I.; Aguzzi, C. Appl Clay Sci 2010, 48, 291.
9. Aguzzi, C.; Cerezo, P.; Viseras, C.; Caramella, C. Appl Clay Sci 2007, 36, 22.
10. Thatiparti, T. R.; Tammishetti, S.; Nivasu, M. V. J Biomed Mater Res B 2010, 92B, 111.
11. Lee, W. F.; Chen, Y. C. J Appl Polym Sci 2004, 91, 2934.
12. Shawky, H. A. J Appl Polym Sci 2011, 119, 2371.
13. Viseras, C.; Aguzzi, C.; Cerezo, P.; Bedmar, M. C. Mater Sci Technol 2008, 24, 1020.
14. Lee, W. F.; Chen, Y. C. J Appl Polym Sci 2005, 98, 1572.
15. Wang, X. Y.; Du, Y. M.; Luo, J. W. Nanotechnology 2008, 19, 1.
16. Wang, X. Y.; Du, Y. M.; Luo, J. W.; Lin, B. F.; Kennedy, J. F. Carbohydr Polym 2007, 69, 41.
17. Zhang, J. P.; Wang, Q.; Xie, X. L.; Li, X.; Wang, A. Q. J Biomed Mater Res B 2010, 92B, 205.
18. Allen, T. C.; Cuculo, J. A. J Polym Sci Macromol Rev 1973, 7, 18.
19. Garrett, Q.; Xu, S. J.; Simmons, P. A.; Vehige, J.; Xie, R. Z.; Kumar, A.; Flanagan, J. L.; Zhao, Z. J.; Willcox, M. D. P. Curr Eye Res 2008, 7, 567.
20. Mao, B. W.; Zhao, A. G.; Huang, M. Y.; Jiang, Y. Y. Polym Adv Technol 2000, 11, 250.
21. Wang, M.; Xu, L.; Hu, H.; Zhai, M. L.; Peng, J.; Nho, Y. C.; Li, J. Q.; Wei, G. S. Nucl Instrum Meth B 2007, 265, 385.
22. Rokhade, A. P.; Agnihotri, S. A.; Patil, S., A.; Mallikarjuna, N. N.; Kulkarni, P. V.; Aminabhavi, T. M. Carbohydr Polym 2006, 65, 243.
23. Almasi, H.; Ghanbarzadeh, B.; Entezami, A. A. Int J Biol Macromol 2010, 46, 1.
24. Wang, W. B.; Wang, A. Q. Carbohydr Polym 2010, 82, 83.
25. Liu, Y.; Wang, W. B.; Wang, A. Q. Desalination 2010, 259, 258.
26. Pongjanyakul, T.; Sungthongjeen, S.; Puttipipatkhachorn, S. Int J Pharm 2006, 3, 1920.
27. González-Rodríguez, M. L.; Holgado, M. A.; Sánchez-Lafuente, C.; Rabasco, A. M.; Fini, A. Int J Pharm 2002, 232, 225.
28. Lin, J. M.; Wu, J. H.; Yang, Z. F.; Pu, M. L. Macromol Rapid Comm 2001, 22, 422–424.
29. Li, A.; Wang, A. Q.; Chen, J. M. J Appl Polym Sci 2004, 92, 1596.
30. Wang, Q.; Xie, X. L.; Zhang, X. W.; Zhang, J. P.; Wang, A. Q. Int J Biol Macromol 2010, 46, 356.
31. Li, J. F.; Li, Y. M.; Dong, H. P. J Agric Food Chem 2008, 4, 1336.
32. Ritger, P. L.; Peppas, N. A. J Controlled Release 1987, 5, 23.